

Reactions of isonitriles with $[\text{Fe}_3(\text{CO})_{12}]$ and $[\text{Ru}_3(\text{CO})_{12}]$ monitored by electrospray mass spectrometry: structural characterisation of $[\text{Fe}_3(\text{CO})_{10}(\text{CNPh})_2]$ and $[\text{Ru}_4(\text{CO})_{11}(\mu_3\text{-}\eta^2\text{-CNPh})_2(\text{CNPh})]$

Corry Decker, William Henderson, Brian K. Nicholson *

Department of Chemistry, School of Science and Technology, University of Waikato, Private Bag 3105, Hamilton, New Zealand

Received 29 January 2004; accepted 17 February 2004

Abstract

The reactions of $[\text{Fe}_3(\text{CO})_{12}]$ or $[\text{Ru}_3(\text{CO})_{12}]$ with RNC (R = Ph, $\text{C}_6\text{H}_4\text{OMe-}p$ or $\text{CH}_2\text{SO}_2\text{C}_6\text{H}_4\text{Me-}p$) have been investigated using electrospray mass spectrometry. Species arising from substitution of up to six ligands were detected for $[\text{Fe}_3(\text{CO})_{12}]$, but the higher-substituted compounds were too unstable to be isolated. The crystal structure of $[\text{Fe}_3(\text{CO})_{10}(\text{CNPh})_2]$ was determined at 150 and 298 K to show that both isonitrile ligands were *trans* to each other on the same Fe atom. For $[\text{Ru}_3(\text{CO})_{12}]$ substitution of up to three COs was found, together with the formation of higher-nuclearity clusters. $[\text{Ru}_4(\text{CO})_{11}(\text{CNPh})_3]$ was structurally characterised and has a spiked-triangular Ru_4 core with two of the CNPh ligands coordinated in an unusual $\mu_3\text{-}\eta^2$ mode.

© 2004 Elsevier B.V. All rights reserved.

Keywords: Iron carbonyl; Ruthenium carbonyl; Isonitrile; Electrospray mass spectrometry; X-ray crystallography

1. Introduction

$[\text{Fe}_3(\text{CO})_{12}]$ and $[\text{Ru}_3(\text{CO})_{12}]$ have played key roles in the development of cluster chemistry. They have been important examples in the debates about structures and fluxional properties, particularly with respect to Johnson's ligand polyhedron arguments for the adoption of an icosahedral arrangement of CO ligands for the smaller Fe_3 triangle and the larger cube-octahedron arrangement for the Ru_3 core [1]. This leads to the bridged C_{2v} structure for the former but a non-bridged D_{3h} structure for the latter. $[\text{Fe}_3(\text{CO})_{12}]$ has also been the archetypal compound for the sometimes heated arguments concerning the mechanisms for CO-ligand fluxionality [2].

Of all the ligands that most resemble CO, but are clearly distinguished from it, are isonitriles RNC. Replacement of some of the CO ligands of $[\text{M}_3(\text{CO})_{12}]$ with

RNC therefore allows subtle changes that can provide extra information concerning the parent species.

For the iron case, some derivatives were prepared many years ago [3]. The first structurally characterised example was $[\text{Fe}_3(\text{CO})_{11}(\text{CNBu}^t)]$ where the isonitrile ligand occupies an axial position on the unique iron atom of the parent C_{2v} structure [4]. This change is sufficient to give a completely ordered structure rather than the 50:50 disordered form of $[\text{Fe}_3(\text{CO})_{12}]$ [5], presumably because the isonitrile ligand prefers a terminal rather than the bridging position that the "star-of-David" disorder model would require. Subsequently, the di-substituted example $[\text{Fe}_3(\text{CO})_{10}(\text{CNBu})_2]$ was characterised, with both isonitrile ligands on the unique iron atom, one axial and one equatorial [6]. Again, the structure is fully ordered. So far no tri-substituted examples have been structurally characterised, though they are known [7], so the pattern of ligand substitution is undetermined since it cannot be deduced from infrared spectra, nor from NMR spectra because of the CO-fluxionality involved.

For $[\text{Ru}_3(\text{CO})_{12}]$ the situation is reversed. The parent cluster shows no disorder of the metal core [8], whereas

* Corresponding author. Fax: +64-7-838-4219.

E-mail address: b.nicholson@waikato.ac.nz (B.K. Nicholson).

the mono- and di-substituted examples with the CNBu^t ligand are disordered in the “star-of-David” fashion [9–11]. For [Ru₃(CO)₁₁(CNBu^t)] the disorder is temperature-dependent, around 12% at room temperature and 6% at 130 K while at 100 K it becomes fully ordered [9–11].

For [Ru₃(CO)₁₀(CNBu^t)₂] the disorder is 50:50, with the isonitrile ligands attached to different Ru atoms [9].

More recently, Farrugia and Mertes have systematically studied the structures of mono- and di-substituted CNBu^t derivatives of the mixed-metal [Fe₂Ru(CO)₁₂] and [FeRu₂(CO)₁₂] clusters, where the CNBu^t ligands prefer axial positions on a ruthenium atom [12].

It is interesting to note that the five structurally characterised [M₃(CO)₁₁(CNBu^t)] examples (M₃ = Fe₃, Ru₃, Os₃, FeRu₂, Fe₂Ru) [4,9,12,13] make up an unusual set of compounds that are isomorphous, but are not isostructural, since the Fe₃ example is derived from the C_{2v} structure, the Ru₃ example based on a twisted-D_{3h} with a disordered Ru₃ unit (12% at room temperature), and the Os example is twisted-D_{3h} but not disordered. The FeRu₂ compound is also based on a D_{3h} form, with a slightly disordered triangle at 293 K (3.4%) as well as scrambling amongst the metal sites, while the Fe₂Ru is C_{2v} with no disorder. This is most readily understood in terms of Johnson’s model – the almost constant ligand polyhedron determines the crystal packing and hence space group, with the varying metal cores occupying the central hole according to their sizes and ease of rotation within the cage [1]. The work on the structures and fluxionality of all three [M₃(CO)₁₂] members of the iron triad has been reviewed [2].

We have now investigated the reactions of [M₃(CO)₁₂] (M₃ = Fe₃ or Ru₃) with the isonitrile ligands CNC₆H₄OMe-*p*, CNCH₂SO₂C₆H₄Me-*p* (TosMIC) and CNPh. The first two of these were chosen because their potentially protonatable sites were expected to facilitate chemical ionisation of neutral complexes for electrospray mass spectrometry (ESMS) by giving [M + H]⁺ ions (c.f. [14]). However, the simpler ligand CNPh was also found to form complexes which generated ions in the ESMS source, so was included. The emphasis in our studies was the characterisation of reaction mixtures by ESMS, and the detection of more highly substituted species.

2. Experimental

Reactions and manipulations were performed under nitrogen in standard Schlenk equipment, except for preparative chromatography which was carried out expeditiously in air using silica plates (Merck, Silica gel 60G). Petroleum spirits refers to a 60–80 °C fraction. Infrared spectra were recorded on a Digilab FTS40 spectrometer, NMR on a Bruker AC300P machine, and ESMS on a VG Platform II mass spectrometer. Samples

were dissolved or diluted in MeOH (unless otherwise specified) and injected via a Rheodyne valve fitted with a 10 μl sample loop, with a mobile phase flow rate of 0.02 ml min⁻¹. Skimmer cone voltages were kept low to minimise fragmentation, 20 V for positive-ion spectra and 5 V for negative-ion spectra. For the negative-ion spectra, Na[OMe] was added where indicated to aid ionisation [15].

2.1. Reactions of [Fe₃(CO)₁₂] with isonitriles

The general reaction was carried out as follows: [Fe₃(CO)₁₂] (0.5 g, 0.99 mmol) was dissolved in THF (10 ml). The isonitrile (3.97 mmol) was added by syringe or as a solid and the reaction stirred at room temperature for ≈2 h. The course of the reaction was monitored by TLC and aliquots were withdrawn at appropriate time intervals for examination by ESMS.

When the reactions were complete and preliminary ESMS studies had been carried out, the solvent was removed in vacuo. The reaction products were redissolved in a minimum amount of CH₂Cl₂, and chromatographed on silica plates with a solvent mixture of petroleum spirits/CH₂Cl₂ (CNPh derivatives 1:1, CNC₆H₄OMe-*p* derivatives 1:2, TosMIC derivatives 1:2). Yields of the complexes were not determined because only parts of the crude reaction product were used at a time for chromatography, and significant decomposition always accompanied attempted separation. The compounds that survived chromatography were removed from the plates and recrystallised for further characterisation. Satisfactory elemental analyses were obtained for CNPh and TosMIC derivatives, but not for any compounds involving the CNC₆H₄OMe-*p* ligand. The following derivatives were characterised:

2.1.1. [Fe₃(CO)₁₁(CNPh)]

*R*_f = 0.68 (green). Found: C, 37.79; H, 1.31; N, 2.35%. C₁₈H₅Fe₃NO₁₁ requires C, 37.31; H, 0.86; N, 2.42%. IR (CHCl₃): ν(CN) 2153 (m); ν(CO) 2080 (m), 2039 (sh), 2033 (s), 2014 (sh), 1998 (sh) cm⁻¹. ESMS (+ve ion): [M + H]⁺ *m/z* 580 (100%).

2.1.2. [Fe₃(CO)₁₀(CNPh)₂]

*R*_f = 0.49 (green). Found: C, 44.65; H, 1.52; N, 4.14%. C₂₄H₁₀Fe₃N₂O₁₀ requires C, 44.04; H, 1.53; N, 4.28%. IR (pet. spirits): ν(CN) 2150 (w), 2118 (m); ν(CO) 2056 (s), 2030 (sh), 2019 (s), 1996 (sh), 1988 (sh), 1974 (sh) cm⁻¹. ESMS (+ve ion): [M + H]⁺ *m/z* 655 (100%).

2.1.3. [Fe₃(CO)₉(CNPh)₃]

*R*_f = 0.24 (green). Elemental analysis did not give acceptable values, e.g. Found: C, 53.34; H, 3.98; N, 4.51%. C₃₀H₁₅Fe₃N₃O₉ requires C, 49.40; H, 2.08; N, 5.76%. IR (pet. spirits): ν(CN) 2148 (w), 2113 (m);

$\nu(\text{CO})$ 2052 (m), 2038 (m), 2016 (sh), 2009 (s), 1990 (sh), 1978 (sh) cm^{-1} . ESMS (+ve ion): $[\text{M} + \text{H}]^+$ m/z 730 (100%).

2.1.4. $[\text{Fe}_3(\text{CO})_8(\text{CNPh})_4]$

$R_f = 0.09$ (green). IR (CHCl_3): $\nu(\text{CN})$ 2148 (w), 2113 (m); $\nu(\text{CO})$ 2000 (s), 1990 (sh), 1986 (sh), 1965 (sh) cm^{-1} . ESMS (+ve ion): $[\text{M} + \text{H}]^+$ m/z 806 (100%).

2.1.5. $[\text{Fe}_3(\text{CO})_{11}(\text{CNC}_6\text{H}_4\text{OMe-p})]$

$R_f = 0.58$ (green). IR (CHCl_3): $\nu(\text{CN})$ 2157 (br); $\nu(\text{CO})$ 2081 (s), 2057 (sh), 2034 (s), 2041 (sh), 1996 (sh), 1972 (sh) cm^{-1} . ^1H NMR (CDCl_3): δ 7.44 (2H, s, H_2'), δ 6.95 (2H, s, H_3'), δ 3.86 (3H, s, OCH_3). ^{13}C - $\{^1\text{H}\}$ NMR (CDCl_3): δ 212.7 (s, $\underline{\text{CO}}$), δ 160.1 (s, C_4'), δ 126.9 (s, C_2'), δ 114.8 (s, C_3'), δ 55.7 (s, OCH_3). ESMS (+ve ion): $[\text{M} + \text{H}]^+$ m/z 610 (100%).

2.1.6. $[\text{Fe}_3(\text{CO})_{10}(\text{CNC}_6\text{H}_4\text{OMe-p})_2]$

$R_f = 0.21$ (green). Elemental analysis did not give acceptable values, e.g. C, 47.28; H, 2.96; N 3.67%. $\text{C}_{26}\text{H}_{14}\text{Fe}_3\text{N}_2\text{O}_{12}$ requires C, 43.70; H, 0.16; N, 3.92%. IR (CHCl_3): $\nu(\text{CN})$ 2126 (br); $\nu(\text{CO})$ 2059 (s), 2032 (s), 2014 (sh), 1994 (sh), 1989 (sh), 1964 (sh) cm^{-1} . IR (pet. spirits): $\nu(\text{CN})$ 2135 (sh) 2125 (m); $\nu(\text{CO})$ 2057 (s), 2028 (s), 2024 (sh), 2018 (s), 2013 (sh), 1999 (m), 1987 (sh), 1972 (s) cm^{-1} . ^1H NMR (CDCl_3): δ 7.39 (4H, d, $^3J_{\text{H}_2',\text{H}_3'} = 2.5$ Hz, H_2'), δ 6.91 (4H, d, $^3J_{\text{H}_3',\text{H}_2'} = 5.8$ Hz, H_3'), δ 3.85 (3H, s, OCH_3). ESMS (+ve ion): $[\text{M} + \text{H}]^+$ m/z 715 (100%).

2.1.7. $[\text{Fe}_3(\text{CO})_9(\text{CNC}_6\text{H}_4\text{OMe-p})_3]$

$R_f = 0.06$ (green). IR (pet. spirits): $\nu(\text{CN})$ 2120 (m); $\nu(\text{CO})$ 2053 (sh), 2037 (m), 2021 (sh), 2016 (sh), 2006 (s), 2000 (sh), 1991 (sh), 1984 (sh), 1974 (m) cm^{-1} . ESMS (+ve ion): $[\text{M} + \text{H}]^+$ m/z 820 (100%).

2.1.8. $[\text{Fe}_3(\text{CO})_{11}(\text{TosMIC})]$

$R_f = 0.78$ (green). Found: C, 35.94; H, 1.35; N, 2.16%. $\text{C}_{20}\text{H}_9\text{Fe}_3\text{NSO}_{13}$ requires C, 35.77; H, 1.34; N, 2.10%. IR (CHCl_3): $\nu(\text{CN})$ 2173 (m, br); $\nu(\text{CO})$ 2082 (sh), 2062 (s), 2047 (sh), 2003 (sh), 1974 (s) cm^{-1} . ESMS (+ve ion): $[\text{M} + \text{H}]^+$ m/z 672 (100%), $[2\text{M} + \text{H}]^+$ m/z 1344 (10%). ESMS (–ve ion): $[\text{M} - \text{H}]^-$ m/z 670 (20%), $[\text{M} - \text{CO} - \text{H}]^-$ m/z 642 (100%).

2.1.9. $[\text{Fe}_3(\text{CO})_{10}(\text{TosMIC})_2]$

$R_f = 0.63$ (green). Found: C, 39.97; H, 2.13; N, 3.35%. $\text{C}_{28}\text{H}_{18}\text{Fe}_3\text{N}_2\text{S}_2\text{O}_{14}$ requires C, 40.10; H, 2.15; N, 3.34%. IR (CHCl_3): $\nu(\text{CN})$ 2164 (m, br); $\nu(\text{CO})$ 2098 (sh), 2080 (s), 2062 (sh), 2042 (s), 2033 (sh), 2020 (sh) cm^{-1} . ESMS (+ve ion): $[\text{M} + \text{H}]^+$ m/z 839 (100%), $[2\text{M} + \text{H}]^+$ m/z 1677 (5%). ESMS (–ve ion): $[\text{M} - \text{H}]^-$ m/z 837 (57%), $[\text{M} - \text{CO} - \text{H}]^-$ m/z 809 (100%).

2.1.10. $[\text{Fe}_3(\text{CO})_9(\text{TosMIC})_3]$

$R_f = 0.39$ (green). Found: C, 44.18; H, 4.28; N, 3.43%. $\text{C}_{36}\text{H}_{27}\text{Fe}_3\text{N}_3\text{S}_3\text{O}_{15}$ requires C, 42.99; H, 2.69; N, 4.18%. IR (CHCl_3): $\nu(\text{CN})$ 2168 (m, br), 2143 (w); $\nu(\text{CO})$ 2083 (sh), 2074 (sh), 2061 (m), 2030 (s), 2015 (sh), 1991 (sh), 1965 (sh) cm^{-1} . ESMS (+ve ion): $[\text{M} + \text{H}]^+$ m/z 1006 (100%). ESMS (–ve ion): $[\text{M} - \text{H}]^-$ m/z 1004 (100%), $[\text{M} - \text{CO} - \text{H}]^-$ m/z 976 (20%).

2.2. Thermolysis of $[\text{Fe}_3(\text{CO})_{12-n}(\text{CNR})_n]$, $n = 1, 2$

A small amount of $[\text{Fe}_3(\text{CO})_{12-n}(\text{CNR})_n]$, $n = 1, 2$ (20–50 mg) was gently heated in toluene (5 ml) to 75 °C. The reaction was kept at this temperature for ≈ 5 min (higher temperatures or longer reaction times were found to give lower yields by decomposition of the products, as monitored by TLC). The solvent was removed in vacuo. The products were redissolved in a minimum amount of CH_2Cl_2 , and chromatographed on silica plates with a solvent mixture of petroleum spirits/ CH_2Cl_2 (1:1). Yields of the isolated complexes were not determined because only parts of the crude reaction product were used at a time for chromatography and significant decomposition always accompanied separation.

2.2.1. $[\text{Fe}_3(\text{CO})_9(\mu_3\text{-}\eta^2\text{-CNPh})]$

$R_f = 0.83$ (brown). IR (CHCl_3): $\nu(\text{CO})$ 2087 (m), 2055 (sh), 2041 (s), 2033 (s), 2017 (sh), 1996 (sh), 1978 (sh) cm^{-1} . ESMS (MeOH/MeO^- , –ve ion): $[\text{M} + \text{MeO}]^-$ m/z 554 (100%).

Similarly, green $[\text{Fe}_3(\text{CO})_{10}(\text{CNBu})_2]$ was converted to brown $[\text{Fe}_3(\text{CO})_8(\mu_3\text{-}\eta^2\text{-CNPh})(\text{CNPh})]$ after 5 min at 75 °C in toluene. Chromatography gave $[\text{Fe}_3(\text{CO})_8(\mu_3\text{-}\eta^2\text{-CNPh})(\text{CNPh})]$: $R_f = 0.43$ (red). IR (CHCl_3): $\nu(\text{CN})$ 2146 (m), 2107 (m); $\nu(\text{CO})$ 2041 (s), 2023 (sh), 2015 (sh) cm^{-1} . ESMS (MeOH/MeO^- , –ve ion): $[\text{M} + \text{MeO}]^-$ m/z 629 (100%).

Following the same procedure, heating solutions of $[\text{Fe}_3(\text{CO})_{12-n}(\text{CNC}_6\text{H}_4\text{OMe-p})_n]$, $n = 1$ or 2, allowed isolation of the corresponding compounds, respectively:

2.2.2. $[\text{Fe}_3(\text{CO})_9(\mu_3\text{-}\eta^2\text{-CNC}_6\text{H}_4\text{OMe-p})]$

$R_f = 0.73$ (brown). IR (CHCl_3): $\nu(\text{CO})$ 2086 (m), 2059 (w), 2040 (vs), 2031 (vs), 2015 (s), 1995 (m), 1975 (w) cm^{-1} . ESMS (MeOH/MeO^- , –ve ion): $[\text{M} + \text{MeO}]^-$ m/z 584 (100%).

2.2.3. $[\text{Fe}_3(\text{CO})_8(\mu_3\text{-}\eta^2\text{-CNC}_6\text{H}_4\text{OMe-p})(\text{CNC}_6\text{H}_4\text{OMe-p})]$

$R_f = 0.4$ (red–brown). IR (CHCl_3): $\nu(\text{CN})$ 2146 (m); $\nu(\text{CO})$ 2064 (sh), 2058 (m), 2038 (w), 2019 (vs), 1980 (m) cm^{-1} . ESMS (MeOH/MeO^- , –ve ion): $[\text{M} + \text{MeO}]^-$ m/z 689 (100%).

2.3. Reactions of $[Ru_3(CO)_{12}]$ with isonitriles

The general reaction was carried out as follows: $[Ru_3(CO)_{12}]$ (0.5 g, 0.78 mmol) was dissolved in toluene (10 ml). The isonitrile (3.13 mmol) was added by syringe or as a solid and the reaction was gently refluxed for ≈ 30 min. Samples were withdrawn at appropriate time intervals and the course of the reaction monitored by TLC. The solvent was removed in vacuo, the reaction products redissolved in a minimum amount of CH_2Cl_2 , and chromatographed on silica plates with a solvent mixture of petroleum spirits/ CH_2Cl_2 (CNPh derivatives 1:1, CNC_6H_4OMe-p derivatives 1:2). Yields of the isolated complexes were not determined because only parts of the crude reaction product were used at a time for chromatography. The identity of the complexes $[Ru_3(CO)_{10}(CNPh)_2]$ and $[Ru_3(CO)_9(CNPh)_3]$ were confirmed by comparison with the IR frequencies of previously reported analogues.

2.3.1. $[Ru_3(CO)_{11}(CNPh)]$

$R_f = 0.89$ (yellow). IR ($CHCl_3$): $\nu(CN)$ 2158 (m); $\nu(CO)$ 2091 (m), 2049 (s), 2041 (s), 2021 (sh), 2010 (s), 1998 (sh) cm^{-1} ; [Lit [16] $\nu(CO)$ 2080 (m), 2035 (sh), 2020 (s), 2005 (sh), 1992 (s), 1982 (s), 1975 (sh), 1958 (m), 1948 (m), 1843 (m), 1805 (m), 1790 (m) cm^{-1}]. 1H NMR ($CDCl_3$): δ 7.39–7.28 (5H, m, Ph). ESMS (+ve ion): $[M + H]^+$ m/z 716 (100%). ESMS (MeOH/MeO⁻, -ve ion): $[M - 2CO + MeO]^-$ m/z 690 (100%), $[M - 3CO + MeO]^-$ m/z 661 (31%).

2.3.2. $[Ru_3(CO)_{10}(CNPh)_2]$

$R_f = 0.79$ (orange). IR ($CHCl_3$): $\nu(CN)$ 2157 (sh), 2137 (m); $\nu(CO)$ 2066 (m), 2030 (s), 2005 (sh), 1994 (s), 1986 (sh) cm^{-1} ; [Lit [9] for $CNBU^t$ analogue $\nu(CO)$ 2065 (w), 2020 (s), 2007(m), 1996 (s), 1990 (m), 1986 (m) cm^{-1}].

ESMS (+ve ion): $[M + H]^+$ m/z 791 (100%), $[M - CO + H]^+$ m/z 762 (7%). ESMS (MeOH/MeO⁻, -ve ion): $[M + MeO]^-$ m/z 821 (50%), $[M - CO + MeO]^-$ m/z 792 (8%), $[M - 2CO + MeO]^-$ m/z 763 (100%), $[M - 3CO + MeO]^-$ m/z 734 (8%).

2.3.3. $[Ru_3(CO)_9(CNPh)_3]$

$R_f = 0.73$ (red). IR ($CHCl_3$): $\nu(CN)$ 2162 (m), 2140 (m), 2123 (sh); $\nu(CO)$ 2062 (m), 2030 (s), 1997 (m), 1978 (sh) cm^{-1} ; [Lit [9] for $CNBU^t$ analogue: $\nu(CO)$ 2040 (m), 1998 (s), 1971 (s) cm^{-1}]. ESMS (+ve ion): $[M + H]^+$ m/z 866 (100%), $[M - CO + H]^+$ m/z 838 (5%). ESMS (MeOH/MeO⁻, -ve ion): $[M + MeO]^-$ m/z 896 (100%), $[M - 2CO + MeO]^-$ m/z 838 (20%).

2.3.4. $[Ru_3(CO)_{11}(CNC_6H_4OMe-p)]$

$R_f = 0.95$ (yellow). IR ($CHCl_3$): $\nu(CN)$ 2161 (m); $\nu(CO)$ 2092 (m), 2048 (s), 2041 (s), 2020 (sh), 2009 (s), 1996 (sh) cm^{-1} ; [Lit [9] $\nu(CN)$ 2155 (w); $\nu(CO)$ 2092 (w),

2071 (vw), 2062 (w), 2049 (s), 2041 (vs), 2019 (w), 1999 (m), 1992 (m) cm^{-1}]. ESMS (+ve ion): $[M + H]^+$ m/z 745 (100%), $[M - CO + H]^+$ m/z 719 (30%). ESMS (MeOH/MeO⁻, -ve ion): $[M - 2CO + MeO]^-$ m/z 719 (100%), $[M - 3CO + MeO]^-$ m/z 690 (18%).

2.3.5. $[Ru_3(CO)_{10}(CNC_6H_4OMe-p)_2]$

$R_f = 0.78$ (yellow). IR ($CHCl_3$): $\nu(CN)$ 2159 (sh), 2142 (m); $\nu(CO)$ 2067 (m), 2029 (s), 2004 (sh), 1993 (s), 1980 (sh) cm^{-1} ; [Lit [9] $\nu(CN)$ 2154 (w); $\nu(CO)$ 2093 (m), 2066 (m), 2048 (s), 2040 (s), 2030 (vs), 2022 (s), 1997 (s), 1990 (s) cm^{-1}]. ESMS (+ve ion): $[M + H]^+$ m/z 851 (100%), $[M - CO + H]^+$ m/z 822 (5%). ESMS (MeOH/MeO⁻, -ve ion): $[M + MeO]^-$ m/z 881 (28%), $[M - CO + MeO]^-$ m/z 853 (12%), $[M - 2CO + MeO]^-$ m/z 822 (100%).

2.4. Synthesis of $[Ru_4(CO)_{11}(CNPh)_3]$

$[Ru_3(CO)_{12}]$ (0.5 g, 0.78 mmol) was dissolved in toluene (10 ml). CNPh (0.32 ml, 3.13 mmol) was added by syringe and the reaction was gently refluxed for ≈ 30 min. The course of the reaction monitored by TLC. The solvent was removed in vacuo, the reaction products redissolved in a minimum amount of CH_2Cl_2 , and chromatographed on silica plates with petroleum spirits/ CH_2Cl_2 (1:1). $[Ru_4(CO)_{11}(CNPh)_3]$ was obtained from the fifth fraction ($R_f = 0.65$, red) after $[Ru_3(CO)_{12}]$, $[Ru_3(CO)_{11}(CNPh)]$, $[Ru_3(CO)_{10}(CNPh)_2]$ and $[Ru_3(CO)_9(CNPh)_3]$. This fraction was a mixture of two compounds (as two close bands that could not be separated by chromatography) and so no elemental analysis was obtained on the solid. IR ($CHCl_3$): $\nu(CN)$ 2166 (m); $\nu(CO)$ 2076 (m), 2050 (s), 2033 (s), 2006 (m), 1985 (sh) cm^{-1} . ESMS (+ve ion): $[M + H]^+$ m/z 1024 (100%).

ESMS (MeOH/MeO⁻, -ve ion): $[M + MeO]^-$ m/z 1053 (100%) {also observed: $[Ru_4(CO)_{12}(CNPh)_2 + MeO]^-$ m/z 976 (33%), $[Ru_4(CO)_{12}(CNPh)_2 - CO + MeO]^-$ m/z 946 (8%), $[Ru_4(CO)_{12}(CNPh)_2 - 2CO + MeO]^-$ m/z 919 (35%)}.

2.5. Synthesis of $[Ru_4(CO)_{11}(CNC_6H_4OMe-p)_3]$

This reaction was carried out in the same manner as for the CNPh analogue and the product fraction had $R_f = 0.53$ (red). This fraction was again a mixture of two compounds, which could not be separated by chromatography, and so no elemental analysis could be obtained. IR ($CHCl_3$): (CN) 2165 (m); $\nu(CO)$ 2075 (m), 2062 (sh), 2058 (sh), 2049 (s), 2032 (vs), 2004 (m), 1981 (w) cm^{-1} . ESMS (MeCN/ H_2O , +ve ion): $[M + H]^+$ m/z 1114, (100%), $[M - CO + H]^+$ m/z 1085, (17%), $[M - CO + MeCN + H]^+$ m/z 1128, (42%), $[M + MeCN + H]^+$ m/z 1155, (28%).

ESMS (MeOH/MeO⁻, -ve ion): $[M + MeO]^-$ m/z 1143, (100%).

Table 1

Crystal data and refinement details for $[\text{Fe}_3(\text{CO})_{10}(\text{CNPh})_2]$ at 293 and 150 K, and for $[\text{Ru}_4(\text{CO})_{11}(\text{CNPh})_3]$

	$[\text{Fe}_3(\text{CO})_{10}(\text{CNPh})_2]$ at 293 K	$[\text{Fe}_3(\text{CO})_{10}(\text{CNPh})_2]$ at 150 K	$[\text{Ru}_4(\text{CO})_{11}(\text{CNPh})_3]$
Empirical formula	$\text{C}_{24}\text{H}_{10}\text{Fe}_3\text{N}_2\text{O}_{10}$	$\text{C}_{24}\text{H}_{10}\text{Fe}_3\text{N}_2\text{O}_{10}$	$\text{C}_{32}\text{H}_{15}\text{N}_3\text{O}_{11}\text{Ru}_4$
Formula mass	653.89	653.89	1021.75
Crystal system	Monoclinic	Monoclinic	Monoclinic
Space group	$P2_1/c$	$P2_1/c$	$P2_1/c$
a (Å)	15.551(1)	15.229(1)	9.4699(1)
b (Å)	14.068(1)	13.913(1)	19.6533(1)
c (Å)	11.975(1)	11.829(2)	18.5984(2)
β (°)	100.81(1)	99.80(1)	102.666(1)
Volume (Å ³)	2573.0(3)	2469.7(1)	3377.20(5)
Temperature (K)	293(2)	150(2)	150(2)
Z	4	4	4
Density (g cm ⁻³)	1.688	1.759	2.010
Absorption coefficient (mm ⁻¹)	1.73	1.80	1.82
$T_{\text{max,min}}$	0.875, 0.627	0.894, 0.711	0.897, 0.712
Total reflections	13,634	12,815	18,284
Unique reflections	4527	4376	6392
R_{int}	0.0357	0.066	0.023
$R_1(I > 2\sigma(I))$	0.0381	0.0551	0.0232
wR_2 (all data)	0.0823	0.1376	0.0488

2.6. X-ray crystal structure determinations

Data were obtained on a Siemens SMART CCD diffractometer operating under standard conditions. Data were corrected for absorption and other effects using an empirical method (SADABS [17]) and the structures were solved and refined on F_o^2 using the SHELX 97 programs [18] manipulated under WinGx [19]. Hydrogen atoms were included in calculated positions. Details are given in Table 1.

3. Results and discussion

3.1. Reactions of isocyanides with $[\text{Fe}_3(\text{CO})_{12}]$

A solution of $[\text{Fe}_3(\text{CO})_{12}]$ with four equivalents of CNPh was stirred at room temperature for 2 h. A sample was extracted, diluted with MeOH and examined by ESMS. This showed a series of major ions that could be readily assigned to the $[\text{M} + \text{H}]^+$ species derived from the substituted cluster $[\text{Fe}_3(\text{CO})_{12-n}(\text{CNPh})_n]$ for $n = 3-5$. There was also a weak peak at m/z 955 which corresponds to $[\text{Fe}_3(\text{CO})_6(\text{CNPh})_6]$. There were no signals in the mixture for the mono- or di-substituted clusters, but this was probably because of poor ability to ionise under the conditions of the experiment, since they were subsequently shown to be present by chromatography. ESMS signals could be obtained from these lower-substituted derivatives in their pure, isolated form but only with concentrated solutions. The ESMS data are therefore useful for indicating which species are present in solution, but cannot be interpreted quantitatively since the relative ease of chemical ionisation is

more important than relative abundance. For the reactions with CNPh it was surprising that ESMS-detectable ions were found at all, since the site for chemical ionisation through protonation is not obvious. Possibly with increasing numbers of isocyanide ligands the basicity of the CO ligands increases (especially the μ -CO ones) to the point where protonation is favoured. An alternative site for ionisation by H^+ is the M–M bonds, as suggested for $[\text{Ru}_3(\text{CO})_9(\text{PPh}_3)_3]$ which also gives strong $[\text{M} + \text{H}]^+$ ions in the ESMS whereas the parent $[\text{Ru}_3(\text{CO})_{12}]$ does not [15].

Chromatography of the reaction mixture allowed separation and full characterisation of the first two members $[\text{Fe}_3(\text{CO})_{12-n}(\text{CNPh})_n]$ for $n = 1, 2$, and spectroscopic characterisation for the next two with $n = 3, 4$. However, the higher derivatives with $n = 5$ or 6 were too fragile for isolation, so rely solely on the ESMS results from the crude reaction mixture for evidence of their existence. These results are consistent with previous work with CNBu^t where $[\text{Fe}_3(\text{CO})_{12-n}(\text{CNBu})_n]$ for $n = 1-3$ were well-characterised, but the $n = 4$ example, the highest-substituted $[\text{Fe}_3(\text{CO})_{12}]$ derivative previously detected, was too unstable even for ¹³C NMR studies [4,6,7]. It is noteworthy that no $[\text{M}_3(\text{CO})_9(\text{CNR})_3]$ compound (M = Fe, Ru) has yet yielded crystals suitable for X-ray analysis.

The equivalent reaction between $[\text{Fe}_3(\text{CO})_{12}]$ and CNR^* ($\text{R}^* = \text{C}_6\text{H}_4\text{OMe-}p$) was more complicated. An initial mass spectrum of the reaction mixture showed not only peaks arising from substitution products $[\text{Fe}_3(\text{CO})_{12-n}(\text{CNR}^*)_n]$ for $n = 3-5$, but also species resulting from cluster fragmentation $[\text{Fe}_2(\text{CO})_{9-n}(\text{CNR}^*)_n]$ ($n = 4,5,6$) and $[\text{Fe}(\text{CO})_{5-n}(\text{CNR}^*)_n]$ ($n = 2-5$). The difference between this system and the CNPh one may be that

CNR* has an –OMe group which can be protonated in the di-iron and mono-iron compounds, so that equivalent compounds may have been invisible in the ESMS in the CNPh experiment. Chromatography of the mixture yielded $[\text{Fe}_3(\text{CO})_{12-n}(\text{CNR}^*)_n]$ for $n = 1-3$. These were characterised by their $[\text{M} + \text{H}]^+$ ions in the ESMS spectra, and by comparison of their $\nu(\text{CO})$ spectra with analogous compounds since analytically pure crystalline samples could not be obtained.

Equivalent reactions using TosMIC provided different results again. The ESMS spectrum of the crude reaction mixture is shown in Fig. 1. There is a clear family of peaks derived from $[\text{Fe}_3(\text{CO})_{12-n}(\text{TosMIC})_n]$ for $n = 1-5$ in this case. There is also another series of peaks which appear to have arisen from addition of a TosMIC ligand, with concomitant oxidation to give $[\text{Fe}_3(\text{CO})_{12}(\text{TosMIC})]^+$, and substituted derivatives thereof. This unusual behaviour was not found with any of the other isonitriles, and chromatography allowed isolation of only $[\text{Fe}_3(\text{CO})_{12-n}(\text{TosMIC})_n]$ for $n = 1-3$ so no further information could be obtained concerning these species.

The positive-ion ESMS for the TosMIC derivatives showed $[\text{M} + \text{H}]^+$ peaks arising from protonation as expected. Less predictably, the negative-ion spectra showed clean peaks assignable to $[\text{M} - \text{H}]^-$ ions formed in situ. Presumably the CH_2 protons of the ligand are rendered acidic enough by the adjacent NC and SO_2 groups to facilitate chemical ionisation in the mass spectrometer by proton removal. This suggests that TosMIC is a versatile ligand for investigation of reactions by ESMS.

In summary, the use of ESMS to monitor reaction mixtures of $[\text{Fe}_3(\text{CO})_{12}]$ and isonitriles provides useful information that is not available by other means. It shows clearly that: (i) the reactions give mixtures of substituted derivatives rather than single products based on the stoichiometry of the reaction; (ii) compounds can be detected with up to six CNR ligands incorporated, even although only those with up to three are stable

enough to be isolated by chromatography; (iii) some fragmentation to give mono- and di-iron compounds occurs and (iv) TosMIC reacts in a more complicated fashion than does CNPh, giving rise to a wider range of products.

3.2. X-ray crystal structure determinations of $[\text{Fe}_3(\text{CO})_{10}(\text{CNPh})_2]$

Crystal structures of the mono- and di-substituted $[\text{Fe}_3(\text{CO})_{12}]$ with CNBu^t have been available since 1982 and 1990, respectively [4,6]. For both, the basic $[\text{Fe}_3(\text{CO})_{12}]$ structure is preserved. In $[\text{Fe}_3(\text{CO})_{11}(\text{CNBu}^t)]$, the isonitrile ligand occupies an axial site on the non-bridged iron atom, while in $[\text{Fe}_3(\text{CO})_{12}(\text{CNBu}^t)_2]$, both isonitrile ligands were found to be on the unique iron atom, one in an axial and the other in an equatorial site, as in **1**. The only other crystal structure of the type $[\text{Fe}_3(\text{CO})_{12-n}(\text{CNR})_n]$ is for $n = 1$ and $\text{R} = \text{CF}_3$, where CNCF_3 occupies one of the two bridging positions of an $[\text{Fe}_3(\text{CO})_{12}]$ structure [20]. There is no disorder of the metal triangle for any of these derivatives.

To provide another example, the structure of $[\text{Fe}_3(\text{CO})_{10}(\text{CNPh})_2]$ was determined at -123°C , using crystals obtained from a concentrated CH_2Cl_2 solution that was slowly cooled to -20°C . The full structure is shown in Fig. 2(a), and selected bond parameters are provided in the caption to the figure.

In the solid state, $[\text{Fe}_3(\text{CO})_{10}(\text{CNPh})_2]$ preserves the basic $[\text{Fe}_3(\text{CO})_{12}]$ geometry. The two CNPh ligands have replaced the two axial CO ligands on the unique iron atom as in **2**. This contrasts with the only other structurally characterised complex of this type, $[\text{Fe}_3(\text{CO})_{10}(\text{CNBu}^t)_2]$, where the two isonitrile ligands (although both coordinated to the unique iron atom) occupy one axial and one equatorial position (**1**) [6]. In terms of electronic preferences, axial positions might be favoured by CNPh because the isonitrile is a weaker π -acceptor base than CO. In order to maximise π -bonding to the

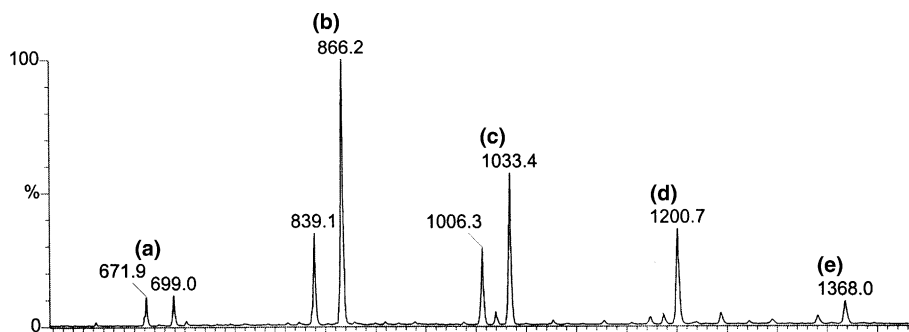


Fig. 1. The positive-ion ESMS of the crude reaction mixture of $[\text{Fe}_3(\text{CO})_{12}]$ and TosMIC, recorded in MeOH. The pairs of peaks correspond to $[\text{Fe}_3(\text{CO})_n(\text{TosMIC})_m + \text{H}]^+$ and $[\text{Fe}_3(\text{CO})_{n+1}(\text{TosMIC})_m]^+$ for (a) $n = 11, m = 1$; (b) $n = 10, m = 2$; (c) $n = 9, m = 3$; (d) $n = 8, m = 4$; (e) $n = 7, m = 5$.

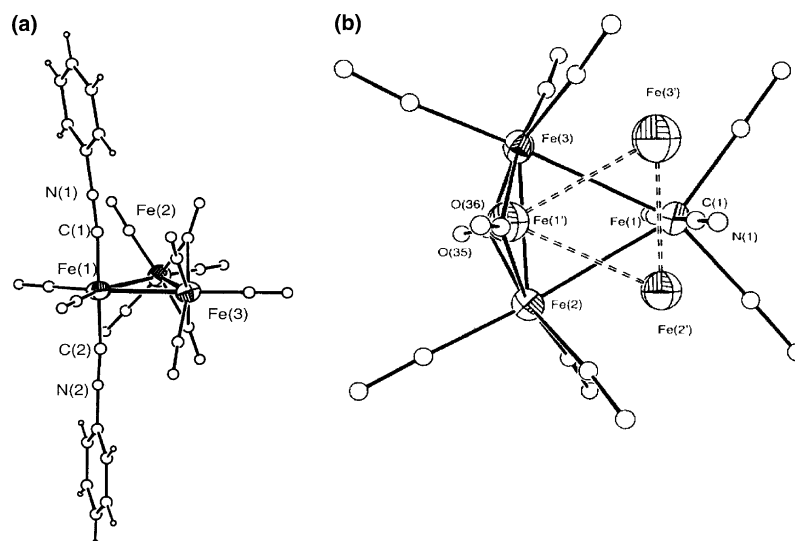


Fig. 2. (a) The structure of $[\text{Fe}_3(\text{CO})_{10}(\text{CNPh})_2]$. (b) The 5% disorder of the Fe_3 triangle found in the determination carried out at 150 K. Selected bond lengths (Å): $\text{Fe}(1)\text{--Fe}(2)$ 2.6921(11), $\text{Fe}(1)\text{--Fe}(3)$ 2.6918(11), $\text{Fe}(2)\text{--Fe}(3)$ 2.5594(11), $\text{Fe}(1)\text{--C}(1)$ 1.871(6), $\text{Fe}(1)\text{--C}(2)$ 1.853(6).

remaining CO ligands, they prefer to be *trans* to Fe–Fe bonds, which is only accomplished if both CNPh occupy axial sites. However the different structures adopted by the examples $[\text{Fe}_3(\text{CO})_{10}(\text{CNR})_2]$ ($\text{R} = \text{Bu}$ or Ph) suggest that these preferences are not stronger than crystal packing effects.

Generally, the effects of the isonitrile ligands of $[\text{Fe}_3(\text{CO})_{10}(\text{CNPh})_2]$ on the rest of the molecule are small. The Fe–Fe bond lengths (2.5594(1) Å bridged, 2.6921(1) and 2.6918(1) Å unbridged) are not significantly different from those observed in $[\text{Fe}_3(\text{CO})_{12}]$ {2.551(2) Å bridged, 2.677(2) and 2.684(2) Å unbridged, recorded at 160 K [5]}. Because the CNPh ligands occupy both axial positions on Fe(1), the Fe(1)–Fe(2) and Fe(1)–Fe(3) bond lengths are equivalent. It is noteworthy that the same observation was made for $[\text{Fe}_3(\text{CO})_{10}(\text{CNBu}^t)_2]$, although the Fe(1)–Fe(2) and Fe(1)–Fe(3) bonds are rendered inequivalent by the equatorial isonitrile ligand. This was considered to be a result of the close similarity in bonding interactions for CO and CNR.

The axial and equatorial Fe–C bond lengths to CO ligands deviate only marginally in $[\text{Fe}_3(\text{CO})_{10}(\text{CNPh})_2]$. The same is true for all other reported isonitrile-substituted derivatives. The μ_2 -CO ligands, unlike in $[\text{Fe}_3(\text{CO})_{12}]$, are not significantly asymmetric. The C≡N distances are equivalent for the two ligands [1.143(6) and 1.155(7) Å], as are the C–N–C angles [176.1(6)° and 176.3(1)°].

Towards the end of the refinement, three major residual peaks formed a triangle rotated 60° from the major Fe_3 -triangle. This was clearly a Star-of-David disorder in the location of the iron atoms, and refinement gave 5% for the second compound, as shown in Fig. 2(b). This was surprising since in all other reported isonitrile-substituted derivatives of $[\text{Fe}_3(\text{CO})_{12}]$ the dis-

order is eliminated. Furthermore, for this disorder a 60° rotation of the iron triangle is required which leads to a structure where the axial isonitrile ligands become bridging, which is normally preferred by the CO rather than the isonitrile ligands (an exception is CNCF_3 [20]). As noted earlier, a small amount of metal site disorder has recently been observed for the mixed-metal species $[\text{FeRu}_2(\text{CO})_{11}(\text{CNBu}^t)]$ and $[\text{FeRu}_2(\text{CO})_{10}(\text{CNBu}^t)_2]$, but not for $[\text{Fe}_2\text{Ru}(\text{CO})_{11}(\text{CNBu}^t)]$ and $[\text{Fe}_2\text{Ru}(\text{CO})_{10}(\text{CNBu}^t)_2]$ [12].

The X-ray structure analysis of $[\text{Fe}_3(\text{CO})_{10}(\text{CNPh})_2]$ was repeated at room temperature to see if the extent of disorder varied with temperature, since previous work with $[\text{Ru}_3(\text{CO})_{11}(\text{CNBu}^t)]$ showed more disorder at higher temperatures, proving it to be dynamic [10,11]. The space group and unit cell were identical at 293 K to those found at low temperature. There were also no significant geometric differences in the structures between the two temperatures. A reported variable temperature X-ray structure analysis of $[\text{Fe}_2\text{Ru}(\text{CO})_{10}(\text{CNBu}^t)_2]$ indicated that the Fe–Fe bond was longer and the C–C bond distances in the Bu^t group were shorter at higher temperature, which was attributed to librational effects [12]. An equivalent effect was not observed for $[\text{Fe}_3(\text{CO})_{10}(\text{CNPh})_2]$.

What was completely unexpected was that the room temperature analysis showed no metal framework disorder. Thermodynamically it is not sensible that there would be less disorder at higher temperatures for a dynamic process. The crystals for the two determinations were from two different batches so that a structure with disorder might have been frozen out by crystal packing interactions, or some twinning of the crystals might have occurred, in the first batch. Another possible explanation is that some $[\text{Fe}_3(\text{CO})_{12}]$ had co-crystallised with $[\text{Fe}_3(\text{CO})_{10}(\text{CNPh})_2]$ in the low

temperature batch. Unfortunately, the crystal used for the room temperature data decomposed before a low-temperature data set on the same crystal could be collected. Examination of a series of $[\text{Fe}_3(\text{CO})_{10}(\text{CNPh})_2]$ crystals would be needed to understand this disorder process. What is clear is that in general study of temperature-dependent disorder should be carried out on one single crystal to avoid possible variations from crystal to crystal.

3.3. Thermolysis of $[\text{Fe}_3(\text{CO})_{12-n}(\text{CNPh})_n]$ ($n = 1, 2$)

Previously it has been reported [4] that $[\text{Fe}_3(\text{CO})_{11}(\text{CNBu}^t)]$ undergoes smooth thermolysis by loss of two CO ligands and conversion of the isonitrile to a $\mu_3\text{-}\eta^2$ bonding mode, as in **3a**. This is still a rare type of isonitrile linkage, the only other example being a niobium cluster, $[\text{Nb}_3\text{Cl}_8(\text{CNBu}^t)_4(\mu_3\text{-}\eta^2\text{-CNBu}^t)]$ [21]. The same reaction was therefore carried out with $[\text{Fe}_3(\text{CO})_{11}(\text{CNPh})]$. Heating to 75 °C converted the green solution to a brown one which ESMS indicated contained **3b**, from a clean $[\text{M} + \text{OMe}]^-$ peak. Chromatography allowed isolation of **3b**. The ESMS spectrum of the pure compound in positive-ion mode showed no evidence for formation of a $[\text{M} + \text{H}]^+$ ion, but the negative ion resulted in a strong $[\text{M} + \text{OMe}]^-$ one. This is not surprising since earlier studies on **3a** showed it was susceptible to nucleophilic but not electrophilic attack at the $\mu_3\text{-C}$ atom [4].

A completely analogous reaction occurred with $[\text{Fe}_3(\text{CO})_{10}(\text{CNPh})_2]$ to give a substituted version of **3b** with one $\mu_3\text{-}\eta^2\text{-CNPh}$ and one terminal one. The complexes $[\text{Fe}_3(\text{CO})_{12-n}(\text{CNC}_6\text{H}_4\text{OMe-}p)_n]$ ($n = 1$ or 2) behaved similarly.

3.4. Reactions of isonitriles with $[\text{Ru}_3(\text{CO})_{12}]$

In previous work, reaction of $[\text{Ru}_3(\text{CO})_{12}]$ with CNBu^t gave $[\text{Ru}_3(\text{CO})_{11}(\text{CNBu}^t)]$ and $[\text{Ru}_3(\text{CO})_{10}(\text{CNBu}^t)_2]$, where substitution was shown to occur progressively on different metal atoms on axial sites and as terminal ligands [9,10]. This differs from phosphine derivatives of $[\text{Ru}_3(\text{CO})_{12}]$, which were found to prefer equatorial sites [22]. The structure of $[\text{Ru}_3(\text{CO})_{12}]$ is not disordered, but many of its derivatives show disorder of the metal framework, e.g. $[\text{Ru}_3(\text{CO})_{10}\{\text{P}(\text{OMe})_3\}_2]$, $[\text{Ru}_3(\text{CO})_{11}(\text{CNBu}^t)]$ and $[\text{Ru}_3(\text{CO})_{10}(\text{PMe}_3)_2]$, but not $[\text{Ru}_3(\text{CO})_{11}\{\text{P}(\text{C}_6\text{H}_{11})_3\}]$. This disorder has been rationalised in terms of a model in which the Ru_3 -triangle occupies two symmetry-related positions while the peripheral atom polyhedron (i.e. the O of the CO ligand and the P of the phosphine or phosphite ligand) remains unchanged [22]. For $[\text{Ru}_3(\text{CO})_{11}(\text{CNBu}^t)]$ and $[\text{Ru}_3(\text{CO})_{11}(\text{PMe}_3)]$, it has also been shown that the disorder is dynamic in origin [11].

Evidence for substitution with isonitriles higher than twofold is still limited. One report briefly mentions the synthesis of the complexes $[\text{Ru}_3(\text{CO})_{12-n}(\text{CNBu}^t)_n]$ ($n = 1\text{--}4$), but without characterisation data [23]. Bruce and co-workers have isolated two tri-substituted complexes but no satisfactory microanalytical data could be obtained [9]. We therefore re-investigated the reactions using ESMS to monitor progress.

When $[\text{Ru}_3(\text{CO})_{12}]$ was gently heated in toluene for 30 min with four equivalents of the isonitrile ligand (CNPh or $\text{CNC}_6\text{H}_4\text{OMe-}p$) and the crude reaction mixtures were injected into the ESMS, none of the expected signals such as $[\text{M} + \text{H}]^+$ ions of $[\text{Ru}_3(\text{CO})_{11}(\text{CNC}_6\text{H}_4\text{OMe-}p)]$ or $[\text{Ru}_3(\text{CO})_{10}(\text{CNC}_6\text{H}_4\text{OMe-}p)_2]$ were observed in positive ion mode. However, in the negative-ion spectrum these two compounds gave strong signals associated with their $[\text{M} + \text{MeO}]^-$ ions. In addition, a weak signal for $[\text{Ru}_3(\text{CO})_9(\text{CNC}_6\text{H}_4\text{OMe-}p)_3 + \text{MeO}]^-$ at m/z 987 was observed. A number of signals associated with higher-nuclearity clusters were also detected. The most intense peaks had a mass difference of 105 amu, reflecting substitution of CO by $\text{CNC}_6\text{H}_4\text{OMe-}p$. From the available information, a cluster series of the type $[\text{Ru}_4(\text{CO})_{12-n}(\text{CNC}_6\text{H}_4\text{OMe-}p)_n]$ ($n = 2\text{--}4$) was tentatively assigned.

Very similar results were obtained for the CNPh derivatives. The most intense ESMS ions were MeO^- adducts derived from $[\text{Ru}_3(\text{CO})_{11}(\text{CNPh})]$ and $[\text{Ru}_3(\text{CO})_{10}(\text{CNPh})_2]$. An equivalent higher-nuclearity series of the type $[\text{Ru}_4(\text{CO})_{14-n}(\text{CNPh})_n]$ ($n = 2\text{--}4$) was also observed.

After separation by chromatography, the products were again analysed by ESMS. Both $[\text{Ru}_3(\text{CO})_{11}(\text{CNR})]$ and $[\text{Ru}_3(\text{CO})_{10}(\text{CNR})_2]$ ionised by methoxide addition as well as by protonation, even though $[\text{M} + \text{H}]^+$ ions had not been observed in the crude reaction solution. The slower-moving bands were of more interest as they represented higher-substituted and/or higher-nuclearity products. In the case of $\text{CNC}_6\text{H}_4\text{OMe-}p$, they were however very close together and could not be separated satisfactorily. Together they gave a signal associated with $[\text{Ru}_3(\text{CO})_9(\text{CNC}_6\text{H}_4\text{OMe-}p)_3 + \text{H}]^+$ as well as from one or more higher-nuclearity clusters such as $[\text{Ru}_4(\text{CO})_{11}(\text{CNC}_6\text{H}_4\text{OMe-}p)_3 + \text{H}]^+$, while $[\text{Ru}_4(\text{CO})_{11}(\text{CNC}_6\text{H}_4\text{OMe-}p)_3 + \text{MeO}]^-$ was the only signal observed in negative-ion mode for the same sample.

For the system involving CNPh , a better separation of the bands occurred. Thus, the bands following the di-substituted complex were isolated and injected into the mass spectrometer. An intense peak corresponding to $[\text{Ru}_3(\text{CO})_9(\text{CNPh})_3 + \text{H}]^+$ was observed in positive-ion mode, while in the negative-ion mode the corresponding $[\text{Ru}_3(\text{CO})_9(\text{CNPh})_3 + \text{MeO}]^-$ ion was also clean.

Isolation of the next-slowest band (which appeared to be a mixture of two species which did not separate) in

the $[\text{Ru}_3(\text{CO})_{12}]/\text{CNPh}$ system, gave a single signal at m/z 1024 in positive-ion, and a number of ions with the most intense at m/z 1054 in negative-ion mode. Presuming the ions to be $[\text{M} + \text{H}]^+$ and $[\text{M} + \text{MeO}]^-$ respectively, the presence of a cluster of formula $[\text{Ru}_4(\text{CO})_{11}(\text{CNPh})_3]$ was indicated. Crystals of $[\text{Ru}_4(\text{CO})_{11}(\text{CNPh})_3]$ (**4**) were obtained for full characterisation. The other component in the mixture is probably $[\text{Ru}_4(\text{CO})_{12}(\text{CNPh})_2]$ from the ESMS data of the mixture, but could not be confirmed.

3.5. X-ray crystal structure determination of $[\text{Ru}_4(\text{CO})_{11}(\text{CNPh})_3]$ (**4**)

Crystals of the cluster $[\text{Ru}_4(\text{CO})_{11}(\text{CNPh})_3]$ were obtained from a concentrated $\text{CH}_2\text{Cl}_2/\text{Et}_2\text{O}$ solution by cooling to -20°C . The structure is shown in Fig. 3 and selected bond parameters are included in the caption. The core geometry of $[\text{Ru}_4(\text{CO})_{11}(\text{CNPh})_3]$ is that of a spiked triangle, a much rarer skeleton for M_4 clusters than tetrahedral or butterfly arrangements. The metal atoms of the triangle each have three terminal CO ligands while the unique ruthenium atom [Ru(4)] is attached to two terminal CO groups and one terminal isonitrile ligand. The remaining two CNPh ligands each bridge a metal–metal bond of the triangle through the isonitrile carbon atom. They also bridge the spike-Ru with a μ_2 -CN bond, as illustrated in Fig. 3. Because of the nature of the bridging ligands, the Ru(1)–Ru(2) and

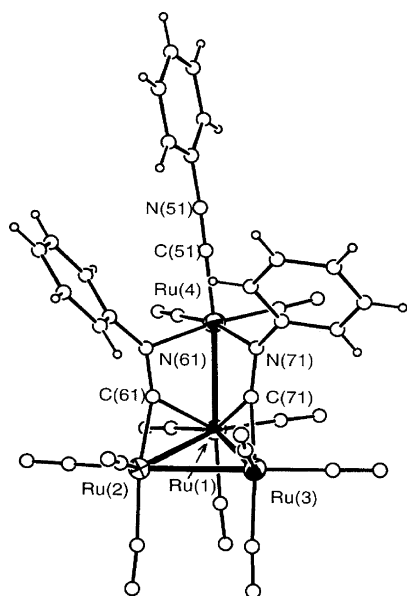


Fig. 3. The structure of $[\text{Ru}_4(\text{CO})_{11}(\text{CNPh})_3]$. Bond lengths (\AA) include: Ru(1)–Ru(2) 2.8341(3), Ru(1)–Ru(3) 2.8226(3), Ru(2)–Ru(3) 2.8895(3), Ru(1)–Ru(4) 2.8258(3), Ru(1)–C(61) 2.172(3), Ru(2)–C(61) 1.962(3), Ru(1)–C(71) 2.127(3), Ru(3)–C(71) 1.966(3), Ru(4)–C(51) 1.994(3), C(51)–N(51) 1.159(3), C(61)–N(61) 1.274(3), C(71)–N(71) 1.270(3).

Ru(1)–Ru(3) bond lengths [2.8341(3) \AA and 2.8226(3) \AA , respectively] are identical. An equivalent bond length was noted for Ru(1)–Ru(4) [2.8258(3) \AA] and is marginally shorter than the unbridged Ru(2)–Ru(3) bond [2.8895(3) \AA]. As a consequence, the bond angles within the Ru-triangle are not quite 60° . The Ru(4)–Ru(1) vector makes an angle of 107° with the basal triangle.

The bonding mode of the two bridging isonitrile ligands is of particular interest. The carbon atoms [C(61) and C(71)] each bridge two metal atoms while the nitrogen atoms [N(61) and N(71)] form a single bond to the unique ruthenium atom Ru(4). This results in a double rather than triple bond between the C and N atoms. The C–N bond lengths [average 1.272(3) \AA] are consistent with this, being longer than in the terminal isonitrile ligand [1.159(3) \AA]. The bonding mode observed can be equated with an imine-type arrangement. The C–N–C [$126.2(2)^\circ$] and C(71)–N(71)–C(72) [$123.6(2)^\circ$] bond angles [average $124.9(2)^\circ$] of the bridging isonitrile ligands also reflect their similarity to imines ($\sim 120^\circ$) rather than that of isonitriles ($\sim 180^\circ$). The terminal isonitrile ligand has an expected C–N–C angle of $177.5(3)^\circ$.

The formal electron count averages 18 for each metal atom; 19 for Ru(1) and Ru(4) and 17 for Ru(2) and Ru(3) atoms. This is calculated assuming the bridging isonitrile ligands each donate one electron to each metal from the carbon atom and two electrons to the unique Ru(4) from the nitrogen atoms. Thus, Ru(1) and Ru(4) are formally electron-rich (19e) whereas Ru(2) and Ru(3) atoms are electron-deficient (17e). This imbalance is partly offset by the μ_2 -C atoms lying closer to Ru(2) or Ru(3) [average 1.964(3) \AA] than to Ru(1) [2.149(3) \AA]. The overall cluster-valence-electron count is 64, as expected for a Ru_4 cluster with four M–M bonds.

$[\text{Ru}_4(\text{CO})_{11}(\text{CNPh})_3]$ is the only reported Ru_4 -isonitrile structure to date. The observed μ_3 - η^2 imine-type bonding mode for isonitrile ligands has been reported before, but only for a small number of other systems. They include Rh_3 , Ru_3 and Os_5 clusters [24].

4. Conclusions

With the ligands used in this study, it has been shown that higher-substituted products do exist for both $[\text{Fe}_3(\text{CO})_{12}]$ (up to sixfold) and $[\text{Ru}_3(\text{CO})_{12}]$ (up to threefold). Even though they become less stable with the degree of substitution, they can still be studied by ESMS. Reactions always seem to give mixtures of products which complicates full characterisation when chromatography leads to decomposition.

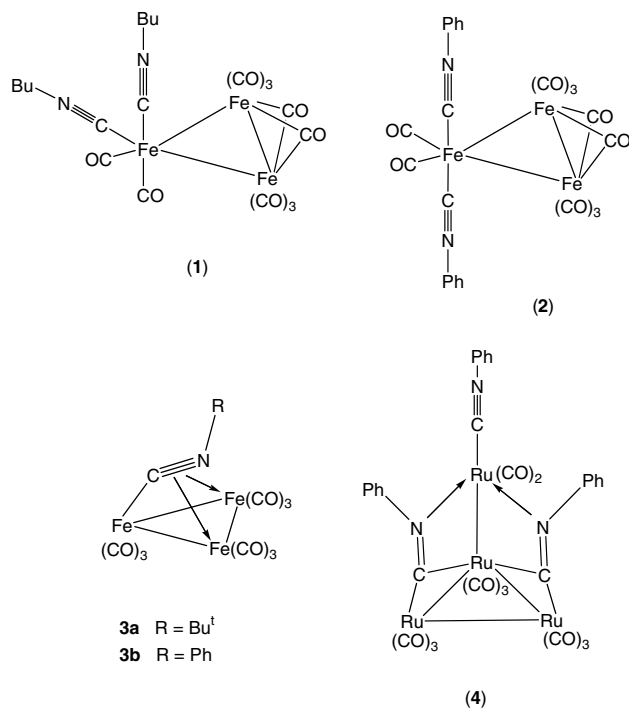
The structure of $[\text{Fe}_3(\text{CO})_{10}(\text{CNPh})_2]$ has been determined and differs from the only other structurally

characterised di-substituted isonitrile derivative of $[\text{Fe}_3(\text{CO})_{12}]$ with respect to the orientations of the isonitrile ligands. The metal framework disorder observed at low temperature is not dynamic in origin, because a separate structure determination at room temperature did not show any disorder.

Pyrolysis reactions of isonitrile derivatives of $[\text{Fe}_3(\text{CO})_{12}]$ led to new analogues of the previously observed species $[\text{Fe}_3(\text{CO})_{9-n}(\mu_3\text{-CNR})(\text{CNR})_m]$ ($m = 0, 1$) as the only major products, extending $\text{R} = \text{Bu}^t$ to $\text{R} = \text{aryl}$ examples. They ionise by formation of $[\text{M} + \text{MeO}]^-$ ions and can be detected readily in the negative-ion mode. The analogous pyrolysis reaction of derivatives of $[\text{Ru}_3(\text{CO})_{12}]$ led to a series of products $[\text{Ru}_4(\text{CO})_{14-n}(\text{CNR})_n]$ ($n = 2-4$) as the only major higher-nuclearity product. $[\text{Ru}_4(\text{CO})_{11}(\text{CNPh})_3]$ represents the only fully characterised isonitrile-substituted ruthenium cluster with four metal atoms.

5. Supplementary material

Full crystallographic data have been deposited with the Cambridge Crystallographic Data Centre, CCDC nos 231171 (**4**), 231172 (**2** at 293 K) and 231173 (**2** at 150 K).



Acknowledgements

We thank Associate Professor Cliff Rickard, University of Auckland, for collection of X-ray intensity data.

References

- R.E. Benfield, B.F.G. Johnson, in: B.F.G. Johnson (Ed.), *Transition Metal Clusters*, Wiley, London, 1980; B.F.G. Johnson, R.E. Benfield, *Topics Stereochem.* 12 (1981) 253.
- B.F.G. Johnson, S. Tay, *Inorg. Chim. Acta* 332 (2002) 201; B.F.G. Johnson, *J. Chem. Soc., Dalton Trans.* (1997) 1473; B.E. Mann, *J. Chem. Soc., Dalton Trans.* (1997) 1457; L.J. Farrugia, *J. Chem. Soc., Dalton Trans.* (1997) 1783; B.E. Hanson, E.C. Lisic, J.T. Petty, G.A. Iannaccone, *Inorg. Chem.* 25 (1986) 4062; D. Lentz, R. Marshall, *Organometallics* 10 (1991) 1487; D. Braga, F. Grepioni, L.J. Farrugia, B.F.G. Johnson, *J. Chem. Soc., Dalton Trans.* (1994) 2911; L.J. Farrugia, A.L. Gillon, D. Braga, F. Grepioni, *Organometallics* 18 (1999) 5022.
- S. Grant, J. Newman, A.R. Manning, *J. Organometal. Chem.* 96 (1975) C11; M.O. Albers, N.J. Coville, T.V. Ashworth, E. Singleton, H.E. Swanepoel, *J. Chem. Soc., Chem. Commun.* (1980) 489.
- M.I. Bruce, T.W. Hambley, B.K. Nicholson, *J. Chem. Soc., Chem. Commun.* (1982) 353; M.I. Bruce, T.W. Hambley, B.K. Nicholson, *J. Chem. Soc., Dalton Trans.* (1983) 2385.
- C.H. Wei, L.F. Dahl, *J. Am. Chem. Soc.* 88 (1966) 1821; C.H. Wei, L.F. Dahl, *J. Am. Chem. Soc.* 91 (1969) 1351; F.A. Cotton, J.M. Troup, *J. Am. Chem. Soc.* 96 (1974) 3070; D. Braga, F. Grepioni, L.J. Farrugia, B.F.G. Johnson, *J. Chem. Soc., Dalton Trans.* (1994) 2911; See also H. Chevreau, C. Martinsky, A. Sevin, C. Minot, B. Silvi, *New J. Chem.* 27 (2003) 1049.
- J.B. Murray, B.K. Nicholson, A.J. Whitton, *J. Organomet. Chem.* 385 (1990) 91.
- X. Chen, B.E. Mann, *Chem. Commun.* (1997) 2233.
- E.R. Corey, L.F. Dahl, *J. Am. Chem. Soc.* 83 (1961) 2203; R. Mason, A.I.M. Rae, *J. Chem. Soc. A* (1968) 778; M.R. Churchill, F.J. Hollander, J.P. Hutchinson, *Inorg. Chem.* 16 (1977) 2655; D. Braga, F. Grepioni, E. Tedesco, P.J. Dyson, C.M. Martin, B.F.G. Johnson, *Trans. Metal Chem.* 20 (1995) 615.
- M.I. Bruce, J.G. Matison, R.C. Wallis, J.M. Patrick, B.W. Skelton, A.H. White, *J. Chem. Soc., Dalton Trans.* (1983) 2365.
- M.I. Bruce, G.N. Pain, C.A. Hughes, J.M. Patrick, B.K. Skelton, A.H. White, *J. Organomet. Chem.* 307 (1986) 343.
- L.J. Farrugia, C. Rosenhahn, S. Whitworth, *J. Cluster Sci.* 9 (1998) 505.
- L.J. Farrugia, P. Mertes, *J. Cluster Sci.* 13 (2002) 199.
- M.I. Bruce, G.N. Pain, C.A. Hughes, J.M. Patrick, B.W. Skelton, A.H. White, *J. Organometal. Chem.* 307 (1986) 343.
- C. Decker, W. Henderson, B.K. Nicholson, *J. Chem. Soc., Dalton Trans.* (1999) 3507.
- W. Henderson, J.S. McIndoe, B.K. Nicholson, P.J. Dyson, *J. Chem. Soc., Dalton Trans.* (1998) 519; W. Henderson, B.K. Nicholson, L.J. McCaffrey, *Polyhedron* 17 (1998) 429.
- C.J. Cardin, D.J. Cardin, N.B. Kelly, G.A. Lawless, M.B. Power, *J. Organometal. Chem.* 341 (1988) 447.
- R.H. Blessing, *Acta Cryst. A* 51 (1995) 33.
- G.M. Sheldrick, *SHELX-97-Programs for X-ray Crystal Structure Determination*, University of Göttingen, 1997.
- WinGX L.J. Farrugia, *J. Appl. Cryst.* 32 (1999) 837. Available from <<http://www.chem.gla.ac.uk/~louis/wingx>>.
- I. Brüdgam, H. Hartl, D. Lentz, *Z. Naturforsch.* 39b (1984) 721.
- F.A. Cotton, W.J. Roth, *J. Am. Chem. Soc.* 105 (1983) 3734.
- M.I. Bruce, J.G. Matison, B.W. Skelton, A.H. White, *J. Chem. Soc., Dalton Trans.* (1983) 2375.

- [23] J.-M. Bassett, D.E. Berry, G.K. Barker, M. Green, J.A.K. Howard, F.G.A. Stone, *J. Chem. Soc. Dalton Trans.* (1979) 1003.
- [24] A.L. Balch, L.A. Fossett, M.M. Olmstead, *Organometallics* 6 (1987) 1827;
O. bin Shawkataly, S.G. Teoh, H.K. Fun, *J. Organometal. Chem.* 464 (1994) C29;
- H. Song, K. Lee, C.H. Lee, J.T. Park, H.Y. Chang, M.G. Choi, *Angew. Chem., Int. Ed. Eng.* 40 (2001) 1500;
H. Song, K. Lee, M.G. Choi, J.T. Park, *Organometallics* 21 (2002) 1756;
H. Song, C.H. Lee, K. Lee, J.T. Park, *Organometallics* 21 (2002) 2514.